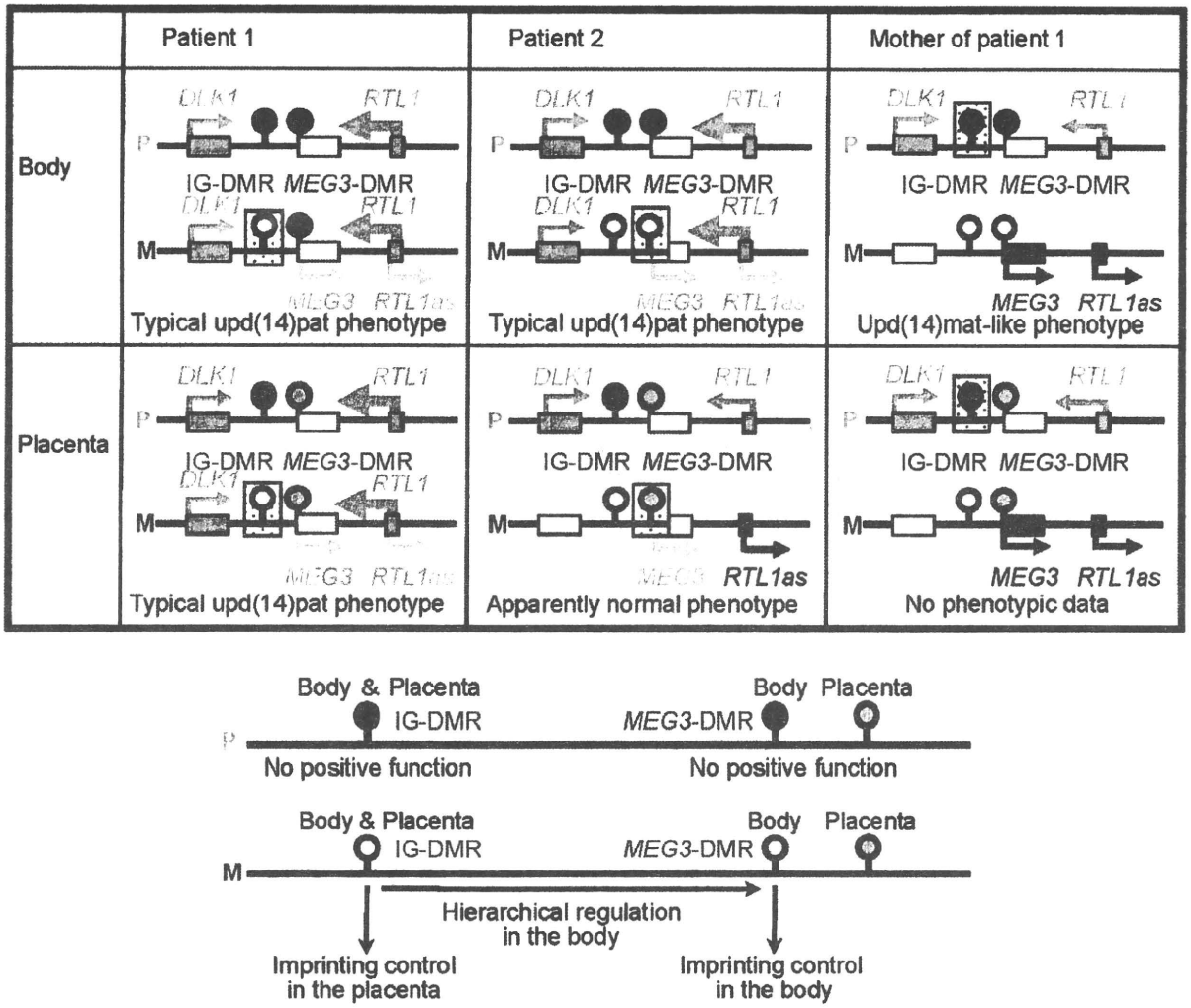

Figure 6. Schematic representation of the observed and predicted methylation and expression patterns. Deleted regions in patients 1 and 2 and the mother of patient 1 are indicated by stippled rectangles. P: paternally derived chromosome; and M: maternally derived chromosome. Representative imprinted genes are shown; these genes are known to be imprinted in the body and the placenta [2] (see also Figure S2). Placental samples have not been obtained in patient 2 and the mother of patient 1 (highlighted with light green backgrounds). Thick arrows for *RTL1* in patients 1 and 2 represent increased *RTL1* expression that is ascribed to loss of functional microRNA-containing *RTL1as* as a repressor for *RTL1* [26,36–38]; this phenomenon has been indicated in placentas with upd(14)pat and in those with an epimutation and a microdeletion involving the two DMRs (Figure S3A and S3C) [2]. *MEG3* and *RTL1as* that are disrupted or predicted to have become silent on the maternally derived chromosome are written in gray. Filled and open circles represent hypermethylated and hypomethylated DMRs, respectively; since the *MEG3*-DMR is rather hypomethylated and regarded as non-DMR in the placenta [2] (see also Figure 3), it is painted in gray.
doi:10.1371/journal.pgen.1000992.g006

Materials and Methods

Ethics statement

This study was approved by the Institutional Review Board Committees at National Center for Child health and Development, University College Dublin, and Dokkyo University School of Medicine, and performed after obtaining written informed consent.

Primers

All the primers utilized in this study are summarized in Table S3.

Sample preparation

For leukocytes and skin fibroblasts, genomic DNA (gDNA) samples were extracted with FlexiGene DNA Kit (Qiagen), and RNA samples were prepared with RNeasy Plus Mini (Qiagen) for *DLK1*, *MEG3*, *RTL1*, *MEG8* and *snoRNAs*, and with mirVana miRNA Isolation Kit (Ambion) for *microRNAs*. For paraffin-embedded tissues including the placenta, brain, lung, heart, liver, spleen, kidney, bladder, and small intestine, gDNA and RNA samples were extracted with RecoverAll Total Nucleic Acids Isolation Kit (Ambion) using slices of 40 μm thick. For fresh control placental samples, gDNA and RNA were extracted using ISOGEN (Nippon Gene). After treating total RNA samples with

Table 2. Clinical and molecular findings in wild-type and PatDi(12) mice and mice with maternally inherited ΔIG-DMR and Δ*Gtl2*-DMR.

	Wildtype	PatDi(12)	ΔIG-DMR (~4.15 kb)[a]	Δ*Gtl2*-DMR (~10 kb)[b]
				Neomycin cassette (+)
<Body>				
Phenotype	Normal	Abnormal[c]	PatDi(12) phenotype[c]	Normal at birth
				Lethal by 4 weeks
Methylation pattern				
IG-DMR	Differential	Methylated	Methylated[d]	Differential
Gtl2-DMR	Differential	Methylated	Epimutated[e]	Methylated[d]
Expression pattern				
Pegs	Monoallelic	Increased (~2x)	Biparental	Grossly normal
			Increased (2x or 4.5x)[f]	
Megs	Monoallelic	Absent	Absent	Decreased (<0.2~0.5x)[g]
<Placenta>				
Phenotype	Normal	Placentomegaly	Apparently normal	Not determined
Methylation pattern				
IG-DMR	Differential	Methylated	Not determined	Not determined
Gtl2-DMR	Non-DMR	Non-DMR	Not determined	Not determined
Expression pattern				
Pegs	Monoallelic	Not determined	Increased (1.5~1.8x)[g]	Decreased (0.5~0.85x)[g]
Megs	Monoallelic	Not determined	Decreased (0.6~0.8x)[g]	Decreased (<0.1~1.0)[g]
Remark			Paternal transmission[h]	Paternal transmission[i]
				Biparental transmission[j]

a The deletion size is smaller than that of patient 1 and her mother in this study, especially at the centromeric region.
b The microdeletion also involves *Gtl2*, and the deletion size is larger than that of patient 2 in this study.
c Body phenotype includes bell-shaped thorax with rib anomalies, distended abdomen, and short and broad neck.
d Hemizygosity for the methylated DMR of paternal origin.
e Hypermethylation of the maternally derived DMR.
f 2x *Dlk1* and *Dio3* expression levels and 4.5x *Rtl1* expression level. The markedly elevated *Rtl1* expression level is ascribed to a synergic effect between activation of the usually silent *Rtl1* of maternal origin and loss of functional microRNA-containing *Rtl1as* as a repressor for *Rtl1* [26,36–38].
g The expression level is variable among examined tissues and examined genes.
h The ΔIG-DMR of paternal origin has permitted normal *Gtl2*-DMR methylation pattern, intact imprinting status, and normal phenotype in the body (no data on the placenta).
i The Δ*Gtl2*-DMR of paternal origin is accompanied by normal methylation pattern of the IG-DMR and variably reduced *Pegs* expression and increased *Megs* expression in the body, and has yielded severe growth retardation accompanied by perinatal lethality.
j The homozygous mutants have survived and developed into fertile adults, despite rather altered expression patterns of the imprinted genes.
doi:10.1371/journal.pgen.1000992.t002

DNase, cDNA samples for *DLK1*, *MEG3*, *MEG8*, and *snoRNAs* were prepared with oligo(dT) primers from 1 μg of RNA using Superscript III Reverse Transcriptase (Invitrogen), and those for *microRNAs* were synthesized from 300 ng of RNA using TaqMan MicroRNA Reverse Transcription Kit (Applied Biosystems). For *RTL1*, cDNA samples were synthesized with *RTL1*-specific primers that do not amplify *RTL1as*. Control gDNA and cDNA samples were extracted from adult leukocytes and neonatal skin fibroblasts purchased from Takara Bio Inc. Japan, and from a fresh placenta of 38 weeks of gestation. Metaphase spreads were prepared from leukocytes and skin fibroblasts using colcemide (Invitrogen).

Structural analysis

Microsatellite analysis and SNP genotyping were performed as described previously [2]. For FISH analysis, metaphase spreads were hybridized with a 5,104 bp FISH-1 probe and a 5,182 bp FISH-2 probe produced by long PCR, together with an RP11-566I2 probe for 14q12 used as an internal control [2]. The FISH-1 and FISH-2 probes were labeled with digoxigenin and detected by rhodamine anti-digoxigenin, and the RP11-566I2 probe was labeled with biotin and detected by avidin conjugated to fluorescein isothiocyanate. For quantitative real-time PCR analysis, the relative copy number to RNaseP (catalog No: 4316831, Applied Biosystems) was determined by the Taqman real-time PCR method using the probe-primer mix on an ABI PRISM 7000 (Applied Biosystems). To determine the breakpoints of microdeletions, sequence analysis was performed for long PCR products harboring the fusion points, using serial forward primers on the CEQ 8000 autosequencer (Beckman Coulter). Direct sequencing was also performed on the CEQ 8000 autosequencer. Oligoarray comparative genomic hybridization was performed with 1×244K Human Genome Array (catalog No: G4411B) (Agilent Technologies), according to the manufacturer's protocol.

Methylation analysis

Methylation analysis was performed for gDNA treated with bisulfite using the EZ DNA Methylation Kit (Zymo Research). After PCR amplification using primer sets that hybridize both methylated and unmethylated clones because of lack of CpG

dinucleotides within the primer sequences, the PCR products were digested with appropriate restriction enzymes for combined bisulfite restriction analysis. For bisulfite sequencing, the PCR products were subcloned with TOPO TA Cloning Kit (Invitrogen) and subjected to direct sequencing on the CEQ 8000 auto-sequencer.

Expression analysis

Standard RT-PCR was performed for *DLK1*, *RTL1*, *MEG3*, *MEG8*, and *snoRNAs* using primers hybridizing to exonic or transcribed sequences, and one μl of PCR reaction solutions was loaded onto Gel-Dye Mix (Agilent). Taqman real-time PCR was carried out using the probe-primer mixtures (assay No: Hs00292028 for *MEG3* and Hs00419701 for *MEG8*; assay ID: 001028 for *miR433*, 000452 for *miR127*, 000568 for *miR379*, and 000477 for *miR154*) on the ABI PRISM 7000. Data were normalized against *GAPDH* (catalog No: 4326317E) for *MEG3* and *MEG8* and against *RNU48* (assay ID: 0010006) for the remaining *miRs*. The expression studies were performed three times for each sample.

To examine the imprinting status of *MEG3* in the leukocytes of the mother of patient 1, direct sequence data for informative cSNPs were compared between gDNA and cDNA. To analyze the imprinting status of *RTL1* in the placental sample of patient 1 and that of *DLK1* in the pituitary and adrenal samples of patient 2, RT-PCR products containing exonic cSNPs informative for the parental origin were subcloned with TOPO TA Cloning Kit, and multiple clones were subjected to direct sequencing on the CEQ 8000 autosequencer. Furthermore, *MEG3* expression pattern was examined using leukocyte gDNA and cDNA samples from multiple normal subjects and leukocyte gDNA samples from their mothers, and *RTL1* expression pattern was analyzed using gDNA and cDNA samples from multiple fresh normal placentas and leukocyte gDNA from the mothers.

Supporting Information

Figure S1 Structural analysis. (A) Quantitative real-time PCR analysis (q-PCR) for four regions (q-PCR-1-4) in patient 2. The q-PCR-1 and q-PCR-2 regions are present in two copies whereas q-PCR-3 and q-PCR-4 regions are present in a single copy in patient 2. The four regions are present in two copies in the parents and a control subject, in a single copy in the two previously reported patients with microdeletions involving the examined regions (Deletion-1 and Deletion-2 are case 2 and case 3 in Kagami et al. [2], respectively), and in three copies in a hitherto unreported case with 46,XX,der(17)t(14;17)(q32.2;p13)pat who have three copies of the 14q32.2 imprinted region. Since the microsatellite locus *D14S985* is present in two copies (Table S1) and the *MEG3*-DMR is deleted (Figure 2) in patient 2, this has served to localize the breakpoints. (B) Oligoarray comparative genomic hybridization for a ~1 Mb imprinted region. All the signals remain within the normal range (-1 SD ~ +1 SD) (shaded in light blue) in patients 1 and 2.
Found at: doi:10.1371/journal.pgen.1000992.s001 (1.17 MB TIF)

Figure S2 Expression analysis. (A) Maternal *MEG3* expression in the leukocytes of normal subjects. Genotyping has been performed for three cSNPs using genomic DNA (gDNA) and cDNA of leukocytes from control subjects and gDNA samples of their mothers, indicating that both maternally and non-maternally (paternally) derived alleles are delineated in the gDNA, whereas maternally inherited alleles alone are identified in cDNA. These three cSNPs have also been studied in the mother of patient 1 (Figure 5D). (B) Paternal *RTL1* expression in the placenta of a normal subject. Genotyping has been carried out for *RTL1* cSNP using gDNA and cDNA samples of a fresh placenta and gDNA sample from the mother, showing that both maternally and non-maternally (paternally) derived alleles are delineated in the gDNA, whereas a non-maternally (paternally) inherited allele alone is detected in cDNA. This cSNP has also been examined in the placenta of patient 1 (Figure 5E). Furthermore, the results confirm that the primers utilized in this study have amplified *RTL1*, but not *RTL1as*.
Found at: doi:10.1371/journal.pgen.1000992.s002 (0.39 MB TIF)

Figure S3 Schematic representation of the observed and predicted methylation and expression patterns in previously reported cases with upd(14)pat/mat-like phenotypes and in normal and upd(14)pat/mat subjects. For the explanations of the illustrations, see the legend for Figure 6. Previous studies have indicated that (1) Epimutation-1, Deletion-1, Deletion-2, and Deletion-3 lead to maternal to paternal epigenotypic alteration; (2) Epimutation-2 results in paternal to maternal epigenotypic alteration; and (3) Deletion-4 and Deletion-5 have no effect on the epigenotypic status [2,5–8,26]. (A) Cases with typical or mild upd(14)pat phenotype. Epimutation-1: Hypermethylation of the IG-DMR and the *MEG3*-DMR of maternal origin in the body, and that of the IG-DMR of maternal origin in the placenta (the *MEG3*-DMR is rather hypomethylated in the placenta) (cases 6–8 in Kagami et al. [2]). Deletion-1: Microdeletion involving *DLK1*, the two DMRs, and *MEG3* on the maternally inherited chromosome (case 2 in Kagami et al. [2]). Deletion-2: Microdeletion involving *DLK1*, the two DMRs, *MEG3*, *RTL1*, and *RTL1as* on the maternally inherited chromosome (cases 3 and 5 in Kagami et al. [2]). Deletion-3: Microdeletion involving the two DMRs, *MEG3*, *RTL1*, and *RTL1as* on the maternally inherited chromosome (case 4 in Kagami et al. [2]). These findings are explained by the following notions: (1) Epimutation (hypermethylation) of the normally hypomethylated IG-DMR of maternal origin directly results in paternalization of the imprinted region in the placenta and indirectly leads to paternalization of the imprinted region in the body via epimutation (hypermethylation) of the usually hypomethylated *MEG3*-DMR of maternal origin. Thus, the epimutation (hypermethylation) is predicted to have impaired the IG-DMR as the primary target, followed by the epimutation (hypermethylation) of the *MEG3*-DMR after fertilization; (2) Loss of the hypomethylated *MEG3*-DMR of maternal origin leads to paternalization of the imprinted region in the body; and (3) Loss of the hypomethylated IG-DMR of maternal origin results in paternalization of the imprinted region in the placenta. Furthermore, epigenotype-phenotype correlations imply that the severity of upd(14)pat phenotype is primarily determined by the *RTL1* expression dosage rather than the *DLK1* expression dosage [2]. (B) Cases with upd(14)mat-like phenotype. Epimutation-2: Hypomethylation of the IG-DMR and the *MEG3*-DMR of paternal origin (Temple et al. [5], Buiting et al. [6], Hosoki et al. [7], and Zechner et al. [8]). Deletion-4: Microdeletion involving *DLK1*, the two DMRs, and *MEG3* on the paternally inherited chromosome (cases 9 and 10 in Kagami et al. [2]). Deletion-5: Microdeletion involving *DLK1*, the two DMRs, *MEG3*, *RTL1*, and *RTL1as* on the paternally inherited chromosome (case 11 in Kagami et al. [2] and patient 3 in Buiting et al. [6]). These findings are consistent with the following notions: (1) Epimutation (hypomethylation) of the normally hypermethylated IG-DMR of paternal origin directly results in maternalization of the imprinted region in the placenta and indirectly leads to maternalization of the imprinted region in the body through epimutation (hypomethylation) of the usually hypermethylated *MEG3*-DMR of paternal origin. Thus, epimutation (hypomethylation) is predicted to have affected the IG-DMR

as the primary target, followed by the epimutation (hypomethylation) of the *MEG3*-DMR after fertilization; and (2) Loss of the hypermethylated DMRs of paternal origin has no effect on the imprinting status [2,26], so that upd(14)mat-like phenotype is primarily ascribed to the additive effects of loss of functional *DLK1* and *RTL1* from the paternally derived chromosome (the effects of loss of *DIO3* appears to be minor, if any [2,35]). Although the *MEGs* expression dosage is predicted to be normal in Deletion-4 and Deletion-5 and doubled in Epimutation-2 as well as in upd(14)mat, it remains to be determined whether the difference in the *MEGs* expression dosage has major clinical effects or not. (C) Normal and upd(14)pat/mat subjects.
Found at: doi:10.1371/journal.pgen.1000992.s003 (2.72 MB TIF)

Table S1 The results of microsatellite and SNP analyses.
Found at: doi:10.1371/journal.pgen.1000992.s004 (0.19 MB DOC)

Table S2 Clinical features in the mother of patient 1.
Found at: doi:10.1371/journal.pgen.1000992.s005 (0.09 MB DOC)

Table S3 Primers utilized in the present study.
Found at: doi:10.1371/journal.pgen.1000992.s006 (0.14 MB DOC)

Author Contributions

Conceived and designed the experiments: MK ACFS TO. Performed the experiments: MK MF KM FK. Analyzed the data: MK TO. Contributed reagents/materials/analysis tools: MJO AJG YW OA NM KM TO. Wrote the paper: TO.

References

1. da Rocha ST, Edwards CA, Ito M, Ogata T, Ferguson-Smith AC (2008) Genomic imprinting at the mammalian Dlk1-Dio3 domain. Trends Genet 24: 306–316.
2. Kagami M, Sekita Y, Nishimura G, Irie M, Kato F, et al. (2008) Deletions and epimutations affecting the human 14q32.2 imprinted region in individuals with paternal and maternal upd(14)-like phenotypes. Nat Genet 40: 237–242.
3. Kagami M, Yamazawa K, Matsubara K, Matsuo N, Ogata T (2008) Placentomegaly in paternal uniparental disomy for human chromosome 14. Placenta 29: 760–761.
4. Kotzot D (2004) Maternal uniparental disomy 14 dissection of the phenotype with respect to rare autosomal recessively inherited traits, trisomy mosaicism, and genomic imprinting. Ann Genet 47: 251–260.
5. Temple IK, Shrubb V, Lever M, Bullman H, Mackay DJ (2007) Isolated imprinting mutation of the DLK1/GTL2 locus associated with a clinical presentation of maternal uniparental disomy of chromosome 14. J Med Genet 44: 637–640.
6. Buiting K, Kanber D, Martin-Subero JI, Lieb W, Terhal P, et al. (2008) Clinical features of maternal uniparental disomy 14 in patients with an epimutation and a deletion of the imprinted DLK1/GTL2 gene cluster. Hum Mutat 29: 1141–1146.
7. Hosoki K, Ogata T, Kagami M, Tanaka T, Saitoh S (2008) Epimutation (hypomethylation) affecting the chromosome 14q32.2 imprinted region in a girl with upd(14)mat-like phenotype. Eur J Hum Genet 16: 1019–1023.
8. Zechner U, Kohlschmidt N, Rittner G, Darnatova N, Beyer V, et al. (2009) Epimutation at human chromosome 14q32.2 in a boy with a upd(14)mat-like clinical phenotype. Clin Genet 75: 251–258.
9. Li E, Beard C, Jaenisch R (1993) Role for DNA methylation in genomic imprinting. Nature 366: 362–365.
10. Rosa AL, Wu YQ, Kwabi-Addo B, Coveler KJ, Reid Sutton V, et al. (2005) Allele-specific methylation of a functional CTCF binding site upstream of MEG3 in the human imprinted domain of 14q32. Chromosome Res 13: 809–818.
11. Wylie AA, Murphy SK, Orton TC, Jirtle RL (2000) Novel imprinted DLK1/GTL2 domain on human chromosome 14 contains motifs that mimic those implicated in IGF2/H19 regulation. Genome Res 10: 1711–1718.
12. Tierling S, Dalbert S, Schoppenhorst S, Tsai CE, Oliger S, et al. (2007) High-resolution map and imprinting analysis of the Gtl2-Dnchc1 domain on mouse chromosome 12. Genomics 87: 225–235.
13. Takada S, Paulsen M, Tevendale M, Tsai CE, Kelsey G, et al. (2002) Epigenetic analysis of the Dlk1-Gtl2 imprinted domain on mouse chromosome 12: implications for imprinting control from comparison with Igf2-H19. Hum Mol Genet 11: 77–86.
14. Ohlsson R, Renkawitz R, Lobanenkov V (2001) CTCF is a uniquely versatile transcription regulator linked to epigenetics and disease. Trends Genet 17: 520–527.
15. Hark AT, Schoenherr CJ, Katz DJ, Ingram RS, Levorse JM, et al. (2000) CTCF mediates methylation-sensitive enhancer-blocking activity at the H19/Igf2 locus. Nature 405: 486–489.
16. Kanduri C, Pant V, Loukinov D, Pugacheva E, Qi CF, et al. (2000) Functional association of CTCF with the insulator upstream of the H19 gene is parent of origin-specific and methylation-sensitive. Curr Biol 10: 853–856.
17. da Rocha ST, Tevendale M, Knowles E, Takada S, Watkins M, et al. (2007) Restricted co-expression of Dlk1 and the reciprocally imprinted non-coding RNA, Gtl2: implications for cis-acting control. Dev Biol 306: 810–823.
18. Wan LB, Pan H, Hannenhalli S, Cheng Y, Ma J, et al. (2008) Maternal depletion of CTCF reveals multiple functions during oocyte and preimplantation embryo development. Development 135: 2729–2738.
19. Ideraabdullah FY, Vigneau S, Bartolomei MS (2008) Genomic imprinting mechanisms in mammals. Mutat Res 647: 77–85.
20. Fitzpatrick GV, Pugacheva EM, Shin JY, Abdullaev Z, Yang Y, et al. (2007) Allele-specific binding of CTCF to the multipartite imprinting control region KvDMR1. Mol Cell Biol 27: 2636–2647.
21. Horsthemke B, Wagstaff J (2008) Mechanisms of imprinting of the Prader-Willi/Angelman region. Am J Med Genet A 146A: 2041–2052.
22. Lin SP, Coan P, da Rocha ST, Seitz H, Cavaille J, et al. (2007) Differential regulation of imprinting in the murine embryo and placenta by the Dlk1-Dio3 imprinting control region. Development 134: 417–426.
23. Coan PM, Burton GJ, Ferguson-Smith AC (2005) Imprinted genes in the placenta–a review. Placenta 26 Suppl A: S10–20.
24. Georgiades P, Watkins M, Surani MA, Ferguson-Smith AC (2000) Parental origin-specific developmental defects in mice with uniparental disomy for chromosome 12. Development 127: 4719–4728.
25. Takada S, Tevendale M, Baker J, Georgiades P, Campbell E, et al. (2000) Delta-like and gtl2 are reciprocally expressed, differentially methylated linked imprinted genes on mouse chromosome 12. Curr Biol 10: 1135–1138.
26. Lin SP, Youngson N, Takada S, Seitz H, Reik W, et al. (2003) Asymmetric regulation of imprinting on the maternal and paternal chromosomes at the Dlk1-Gtl2 imprinted cluster on mouse chromosome 12. Nat Genet 35: 97–102.
27. Takahashi N, Okamoto A, Kobayashi R, Shirai M, Obata Y, et al. (2009) Deletion of Gtl2, imprinted non-coding RNA, with its differentially methylated region induces lethal parent-origin-dependent defects in mice. Hum Mol Genet 18: 1879–1888.
28. Lewis A, Mitsuya K, Umlauf D, Smith P, Dean W, et al. (2004) Imprinting on distal chromosome 7 in the placenta involves repressive histone methylation independent of DNA methylation. Nat Genet 36: 1291–1295.
29. Umlauf D, Goto Y, Cao R, Cerqueira F, Wagschal A, et al. (2004) Imprinting along the Kcnq1 domain on mouse chromosome 7 involves repressive histone methylation and recruitment of Polycomb group complexes. Nat Genet 36: 1296–1300.
30. Sekita Y, Wagatsuma H, Irie M, Kobayashi S, Kohda T, et al. (2006) Aberrant regulation of imprinted gene expression in Gtl2lacZ mice. Cytogenet Genome Res 113: 223–229.
31. Steshina EY, Carr MS, Glick EA, Yevtodiyenko A, Appelbe OK, et al. (2006) Loss of imprinting at the Dlk1-Gtl2 locus caused by insertional mutagenesis in the Gtl2 5′ region. BMC Genet 7: 44.
32. Charlier C, Segers K, Karim L, Shay T, Gyapay G, et al. (2001) The callipyge mutation enhances the expression of coregulated imprinted genes in cis without affecting their imprinting status. Nat Genet 27: 367–369.
33. Georges M, Charlier C, Cockett N (2003) The callipyge locus: evidence for the trans interaction of reciprocally imprinted genes. Trends Genet 19: 248–252.
34. Moon YS, Smas CM, Lee K, Villena JA, Kim KH, et al. (2002) Mice lacking paternally expressed Pref-1/Dlk1 display growth retardation and accelerated adiposity. Mol Cell Biol 22: 5585–5592.
35. Tsai CE, Lin SP, Ito M, Takagi N, Takada S, et al. (2002) Genomic imprinting contributes to thyroid hormone metabolism in the mouse embryo. Curr Biol 12: 1221–1226.
36. Sekita Y, Wagatsuma H, Nakamura K, Ono R, Kagami M, et al. (2008) Role of retrotransposon-derived imprinted gene, Rtl1, in the feto-maternal interface of mouse placenta. Nat Genet 40: 243–248.
37. Seitz H, Youngson N, Lin SP, Dalbert S, Paulsen M, et al. (2003) Imprinted microRNA genes transcribed antisense to a reciprocally imprinted retrotransposon-like gene. Nat Genet 34: 261–262.
38. Davis E, Caiment F, Tordoir X, Cavaillé J, Ferguson-Smith A, et al. (2005) RNAi-mediated allelic trans-interaction at the imprinted Rtl1/Peg11 locus. Curr Biol 15: 743–749.

Title page

Title page: Original article:

Title: Radiological evaluation of dysmorphic thorax of paternal uniparental disomy14

Osamu Miyazaki [a], Gen Nishimura [b], Masayo Kagami [c], Tsutomu Ogata [c]

[a] Department of Radiology, [c] Division of Clinical Genetics and Molecular Medicine National Center for Child Health and Development. 2-10-1 Okura, Seatagaya-ku, Tokyo, Japan zip code: 157-8535

[b] Dept of Radiology, Tokyo Metropolitan Children's Medical Center 2-8-29 Musashidai, Fuchu-shi, TOKYO, JAPAN zip code: 183-8561

Corresponding author; Osamu Miyazaki

e-mail address; osamu-m@rc4.so-net.ne.jp

fax+81-3-3416-2222 Phone:+81-3-3416-0181

Keywords: UPD14, plain radiograph, coat-hanger sign, bell-shaped thorax

Introduction

Uniparental disomy (UPD) refers to the inheritance of a pair of chromosomes from only one parent. UPD is a relatively common phenomenon. The inheritance of both or parts of both maternal chromosomes (heterodisomic maternal UPD) has been found to become more prevalent as the parental ages become more advanced [1]. It is well established that UPD for chromosomes 6.7.11.14 and 15 is associated with recognized syndromes including Prader-Willi syndrome (maternal UPD15), Angelman syndrome (paternal UPD 15), and Beckwith-Wiedemann syndrome (paternal UPD 11) [2].

The paternal uniparental disomy 14 phenotype (upd(14)pat) is a recently recognized genetic condition that is caused by an aberration of the imprinting center in chromosome 14. The clinical hallmarks of upd(14)pat are thoracic hypoplasia and abdominal wall defect. Mild facial dysmorphism and developmental delay are also noted. In addition, it is currently known that upd(14)pat radiologically presents with a distinctive radiological finding, the "coat-hanger" appearance of the ribs and a bell-shaped thorax [3]. In the past, upd(14)pat was often misdiagnosed as bone dysplasias with thoracic hypoplasia, as in Jeune syndrome [4], because attention was not paid to the morphological differences of the thorax between upd(14)pat and other genetic bone diseases. Previous reports on upd(14)pat have been based on a single case or a limited number of cases. To date, there has been no radiological report involving a large series of upd(14)pat cases. Although a previous report suggested that the dysmorphic thorax in upd(14)pat ameliorated in the mid-childhood period [5], it remains to be determined how the thoracic deformity in upd(14)pat evolves with age. The purpose of this study was to quantitatively determine the differences of the thoracic

deformity between upd(14)pat and other genetic bone diseases and to establish the age-dependent radiological evolution of the thoracic hypoplasia in upd(14)pat.

Materials and Methods

The subjects comprised 11 children (6 girls and 5 boys) with upd(14)pat phenotypes proven on molecular grounds [5.6]. Three of the 11 children had been managed in our hospital, and 8 were referred to our institution for the molecular diagnosis. The molecular diagnoses included 7 cases of paternal uniparental disomy, 2 of microdeletion, and 2 of epimutation. The initial radiographs available for the analysis were obtained in the neonatal period (n = 8), and at 7, 24 and 32 months of age (n = 1, respectively). Sequential radiological evaluation was feasible in 4 of 11 children up to 5 years of age. The study was approved by the institutional review board at national center for child health and development.

To assess for the "coat-hanger" sign, the angle between the 6th posterior rib and the horizontal axis was measured (coat hanger angle, CHA; an upward angle was defined as +, and a downward angle as -). The ratio of the mid- to widest thorax diameter (M/W ratio) was calculated for the bell-shaped thorax (Fig. 1.2). For comparison, both indexes were evaluated in 9 cases with bone dysplasia with thoracic hypoplasia, including thanatophoric dysplasia (n=6), Ellis-van Creveld syndrome (n=2), and asphyxiating thoracic dysplasia (n=1). These cases were selected from our radiology database, and their ages ranged from 21 weeks of gestation to 6 years of age (mean: 11 months of age). Both indexes were also evaluated in 5 children with respiratory distress syndrome (RDS) and without skeletal abnormalities that could be assessed to determine the evolution of the normal thoracic morphology. In the RDS group, serial follow-up

radiographs were available from the neonatal period up to 2 years to 6 years of age (mean; 4.2). The measurement of CHA and M/W ratio was performed using an accessory digital tool from a PACS system (Centricity ™ RA 1000 Ver.3.0, GE healthcare, Milwaukee) on the PACS monitor, or using area and protractor commercial software (Lenara Ver2.21, Vector, Tokyo) on a personal computer monitor. An unpaired two-tailed t-test was used for statistical evaluation.

Results

Clinical and measurement data are summarized in Table 1 and Fig. 3. All 11 children with upd(14)pat showed severe upward sweep of the posterior rib or increased CHA, ranging from +28.5 to 45° (mean ± SD; 35.1° ± 5.2) (Figs. 2, 3). Children with bone dysplasias presented with variable manifestations of the posterior rib, and CHA ranged from -19.8 to 21° (mean ± SD; -3.3 ± 13°) (Figs. 3, 4). The difference in CHA was statistically significant between the upd(14)pat and bone dysplasia groups ($p<0.01$). According to this result, approximately +25° was the estimated cut-off line of CHA to differentiate upd(14)pat from skeletal dysplasias (Fig. 3). The M/W ratio ranged from 58 to 93 % (mean ± SD; 75.4 ± 10) in the upd(14)pat group, while it ranged between 80 and 92 % (mean ± SD; 86.8 ± 3.3) in the skeletal dysplasia group (Fig. 3). The difference an unpaired two-tailed t-test in the M/W ratio was, though statistically significant, less conspicuous than that in CHA ($p<0.05$). There was considerable overlap in the range of the M/W ratio between the upd(14)pat and skeletal dysplasia groups.

The age-dependent evolution of CHA and M/W ratio in the upd(14)pat and RDS groups is shown in Fig. 5. In the 4 children with upd(14)pat, CHA remained unaltered regardless of age, ranging from 25 to 45°. In the RDS group (n=5), CHA was constant regardless of age, ranging from -6.4 to 10° (mean; -0.6) at birth and from -8 to 7.3° thereafter (Fig. 5). The M/W ratio of the upd(14)pat group was smaller than that of the RDS group in the neonatal period. However, it gradually increased with age and finally caught up to that seen in the RDS group (Fig. 6、 7).

Discussion

The clinical manifestations of upd(14)pat have been well established to date. The hallmarks of this condition include a small thorax, laryngomalacia, hypoplastic abdominal wall, short limbs with joint contractures, craniofacial dysmorphism, and mental retardation [2]. In addition, several reports on the prenatal diagnosis of upd(14)pat suggested the common occurrence of polyhydramnios and preterm delivery in upd(14)pat [2.7]. A few reports on upd(14)pat have detailed the radiological manifestations, such as disproportionately short limbs, spurring of lower femoral and upper tibial metaphyses, absent glenoid fossa, shortened iliac wing with flaring, thin and elongated clavicle, hypoplastic scapular neck, kyphoscoliosis, hypoplasia of the maxilla and mandible, a broad nasal bridge, wide sutures and multiple wormian bones of skull, contractures of the wrists with ulnar deviation, and stippled calcification [3.8.9.10]. However, these findings are so mild that alone they do not determine the diagnosis. Instead, the distinctive thoracic deformity in upd(14)pat, termed the "coat-hanger" sign as introduced by Offiah et al [3], enables a definitive diagnosis to be made. Sutton et al described the thoracic deformity of upd(14)pat as "anterior ribs bowed caudally (downward), and posterior portions of the ribs bowed cranially (upward)", and these configurations are combined in the characteristic "coat-hanger" sign of the ribs on the chest radiograph. Sutton et al concluded that the skeletal phenotype in upd(14)pat primarily involves the axial skeleton with little to no effect on the long bones [8]. Very small changes of the long bones in upd(14)pat correspond with those of the mouse model (UPD of the distal segment of mouse chromosome 12) [11]. Consequently it is

assumed that imprinted genes on human chromosome 14 and mouse chromosome 12 play a role in axial skeletal formation and ossification [8,11].

In the subsequent articles on upd(14)pat, all 11 affected children unexceptionally presented with the "coat-hanger" sign [5, 6, 12]. It was thought that the upward posterior rib bowing and downward anterior rib bowing (the "coat-hanger" appearance) in upd(14)pat contrast with horizontally oriented ribs generally seen in disorders with thoracic hypoplasia. Based on the radiological sign along with other radiological findings, it is not difficult to differentiate upd(14)pat from other genetic disorders involving thoracic hypoplasia, such as thanatophoric dysplasia, asphyxiating thoracic dysplasia, and metatropic dysplasia [13]. However, there are several disorders wherein thoracic hypoplasia is the sole radiological hallmark, including Barnes syndrome, Shwachman-Diamond syndrome, and the mildest cases of asphyxiating thoracic hypoplasia. Thus, we thought that quantitative analyses of the "coat-hanger" sign could elucidate how different the thoracic hypoplasia in upd(14)pat is from the thoracic hypoplasia in other genetic disorders, and presumed that the measurement of CHA (mean; 35.1°) and M/W ratio (mean; 75.4%) might be helpful when the diagnosis of upd(14)pat is in question. As comparison groups, we included not only cases of severe bone dysplasias but also RDS. Neonates with RDS may present with a small chest [14], and it is not uncommon for them to undergo repeated examinations of chest radiographs because of the association with chronic lung disease.

Kagami et al reported the age-dependent evolution of the thoracic deformity of upd(14)pat in 2 children [5], which was said to ameliorate in mid-childhood. Their observation corresponded with the improvement of the M/W ratio with age described here. By contrast, however, CHA consistently persisted until mid-childhood. This

finding indicates that the "coat-hanger" sign is still discernable during mid-childhood. Radiological findings are presumed to be the only clue to the presence of upd(14)pat after mid-childhood. Serial radiographs (newborn, 2 years, and 9 years), as illustrated by Cotter et al also warrant our observation [15].

A drawback of this study is that it includes a limited number of cases and available radiographs with uneven qualities, such as chest radiographs with some obliquity and radiographs taken in the supine position in the neonatal period vs. the upright position in childhood. Even taking into account these technical problems, however, we believe that our quantitative analyses, particularly the measurement of the CHA, are a valid way to characterize the distinctive thoracic deformity in upd(14)pat.

Conclusion

The "coat-hanger" sign of upd(14)pat was quantitatively represented by CHA, and was found to be more severe than that seen in other genetic bone diseases and to persist into early childhood; thus, the finding helps in the diagnosis of upd(14)pat even after infancy. By contrast, the bell-shaped thorax represented by M/W ratio was significant only in the neonatal period, and its diagnostic value declined with age.

Table-1 Summary of clinical details, measurement of rib angle, CHA, and M/W ratio

case	sex	age (m.o)	molecular or clinical diagnosis	Rt rib angle (degree)	Lt rib angle (degree)	CHA (degree)	M/W ratio (%)
upd(14)pat patients							
1	f	0	upd	36	31	33.5	80
2	m	0	upd	43	41	42	66
3	m	0	upd	27	46	36.5	80
4	m	7	upd	32	38	35	80
5	m	0	deleiton	27	30	28.5	58
6	f	0	Epimutation	35	23	29	77
7	f	0	Epimutation	48	42	45	65
8	f (45,XX)	0	upd	30	34	32	69
9	f	0	upd	46	32	39	74
10	m	24	upd	28	38	33	87
11	f	32	delition	32	33	32.5	93
mean		5.7		35	35.82	35.1	75.4
TD group patients							
1	m	21GW	TD	-9.9	-13.7	-11.8	80
2	f	6	TD	-3.7	12	1	85.6
3	m	21GW	TD	-11.7	-13.9	-12.8	86
4	unknown	20GW	TD	-19.6	-20	-19.8	86
5	m	0	TD	7	-12	-2.5	87
6	m	21GW	TD	-15	-21	-18	87
7	m	84	ATD	4	2	3	88
8	f	11	EvC	9.6	10.3	9.95	90
9	m	24	EvC	14	28	21	92
mean		11		-2.8	-3.1	-3.3	86.8
RDS patients							
1	m	0	RDS	1.8	4	2.9	90
2	m	0	RDS	1.2	-14	-6.4	81.7
3	m	0	RDS	-6.9	-4.1	-5.2	84

4	m	0	RDS	-6	-2	-4	91
5	f	0	RDS	11.3	8.7	10	85
mean		0		0.28	-1.48	-0.54	86.3

abbreviations; CHA: coat hanger angle, M/W: mid- to widest, GW: gestational week, TD: thanatophoric dysplasia, ATD: asphyxiating thoracic dysplasia, EvC: Ellis-van Creveld syndrome, RDS: respiratory distress syndrome

Age: the age at which time the initial radiograph was available.

References

1. Kotzot D (2004) Advanced parental age in maternal uniparental disomy (UPD): implication for the mechanism of formation. Eur J Hum Genet 12: 343-346

2. Towner D, Yang SP, Shaffer G (2001) Prenatal ultrasound findings in a fetus with paternal uniparental disomy 14Q12-rter. Ultrasound Obstet Gynecol 18: 268-271

3. Offiah AC, Cornette L, Hall CM (2003) Paternal uniparental disomy 14: introducing the "coat-hanger" sign. Pediatr Radiol 33: 509-512.

4. Stevenson DA, Brothman AR, Chen Z, Bayrak-Toydemir P, Longo N (2004) Paternal uniparental disomy of chromosome 14: confirmation of a clinically-recognizable phenotype. Am J Med Genet A 130A:88-91.

5. Kagami M, Nishimura G, Okuyama T, Hayashidani M, Takeuchi T et al (2005) Segmental and full paternal isodisomy for chromosome 14 in three patients: narrowing the critical region and implication for the clinical feature. Am J Med Genet A 138A: 127-132

6. Kurosawa K, Sasaki H, Yamanaka M, Shimizu M, Ito Y, et al (2002) Paternal UPD 14 is responsible for a distinctive malformation complex. Am J Med Genet 110:268-272

7. Yamanaka M, Ishikawa H, Saito K, Maruyama Y, Ozawa K, et al (2010) Prenatal findings of paternal uniparental disomy 14: report of four patients. Am J Med Genet 152A: 789-791

8. Sutton VR, McAlister WH, Bertin TK, Kaffe S, Wang JC, et al (2003) Skeletal defect in paternal uniparental disomy for chromosome 14 are re-capitulated in the mouse model (paternal uniparental disomy 12) Hum Genet 113: 447-451.

9. Mattes J, Whitehead B, Liehr T, Wilkinson I, Bear J, et al (2007) Paternal uniparental isodisomy for chromosome 14 with mosaicism for a supernumerary marker chromosome 14. Am J Med Genet 143A: 2165-2171

10. Irving MD, Bulting K, Kanber D, Donaghue C, Schultz R, et al (2010) Segmental paternal uniparental disomy (patUPD) of 14q32 with abnormal methylation elicites the

characteristic features of complete pat UPD14. Am J Med Genet 152A:1942 - 1950

11. Georgiades P, Watkins M, Surani MA, Ferguson-Smith AC (2000) Parental origin-specific developmental defects in mice with uniparental disomy for chromosome 12. Development 127:4719-4728

12. Kagami M, Sekita Y, Nishimura G, Irie M, Kato F, et al (2008) Deletions and epimutations affecting the human 14q32.2 imprinted region in individuals with paternal and maternal upd(14)-like phenotypes. Nat Genet 40: 237-242

13. Spranger JW (2002) Asphyxiating thoracic dysplasia. In: Spranger JW, Brill PW, Poznanski A (ed) Bone dysplasia, an atlas of genetic disorders of skeletal development 2nd edn. Oxford University Press, New York, pp 125-129

14. Swischuk LW (2004) Chapter 1. Respiratory system; respiratory distress in the newborn. In: Swischuk LE (ed) Imaging of the newborn, infant, and young child, 5th edn. Lippincott Williams& Wilkins, Philadelphia, pp 29-36

15. Cotter PD, Kaffe S, McCurdy LD, Jhaveri M, Willner JP, Hirschhorn K (1997) Paternal uniparental disomy for chromosome 14: a case report and review. Am J Med Genet 70: 74-79

Figure legends

Fig. 1 Diagram of coat-hanger angle and mid/widest ratio

a, b) Coat hanger angle (CHA) refers to the average of the angles between the peak point of both 6th posterior ribs and the horizontal axis. If there is no peak point of the 6th posterior ribs, the center of the ribs is utilized instead. The horizontal axis is defined as a line passing through two points of both 6th cost-vertebral junctions. An upward angle is defined as +, and a downward angle as -. CHA is thought to be a quantitative index of the "coat-hanger" sign.

c) The ratio of mid- to widest thorax (M/W ratio) refers to the ratio of the narrowest diameter of the mid-thorax to the widest diameter of the basal thorax. In most cases with upd(14)pat, the thorax showed medial concavity with the top of approximately the 6th rib (the narrowest mid-thorax) and downward sloping toward the 9th to 11th ribs (the widest basal thorax). M/W ratio is thought to be a quantitative index of dysmorphic bell-shaped thorax.

Fig. 2 Examples of the CHA and M/W ratio

a) The 6th posterior ribs show upward bowing that provides the "coat-hanger" sign. The CHA of this case (patient #7 in Table 1) was 45° (the measurement was 48° for the right and 42° for the left).

b) The M/W ratio was 58% in this case (patient #5 in Table 1). This is an example of severe bell-shaped thorax in upd(14)pat.

Fig. 3 Box plot of CHA and M/W ratio with the median, interquartile interval and range.

Fig. 4 Examples of the thoracic appearance and measurement of bone dysplasias with thoracic hypoplasia

a) Thanatophoric dysplasia type 1 (stillbirth at 21 weeks of gestation). Note a narrow thorax with cupped anterior ends as well as short long bones with metaphyseal cupping. The posterior ribs show downward sloping. The CHA was -18°, and the M/W ratio was 87%. Despite the presence of severe thoracic hypoplasia in thanatophoric dysplasia, its morphology is different from that seen in upd(14)pat (Fig. 2).

b) Ellis-van Creveld syndrome (2 years of age). The thorax appears narrow, and trident appearance of the acetabula is seen. Posterior ribs show upward sloping. The CHA was 21°, and the M/W ratio was 92%. The morphological pattern of the thorax differs from that of upd(14)pat.

Fig. 5 Comparative observation of age-dependent transition of CHA between the upd(14)pat and RDS groups. Individual shapes represent individual patients.

Fig. 6 Comparative observation of age-dependent transition of M/W ratio between the pat-UPD and RDS groups. Individual shapes represent individual patients.

Fig 7 Serial images of the thorax deformity in upd(14)pat

In this case, four images taken at different ages were available: (a) neonatal period, (b) 6 months, (c) 1 year, and (d) 4 years. The CHA was almost consistent regardless of age, while the M/W ratio increased with advancing age. The "coat-hanger" sign and

bell-shaped thorax are readily identifiable in the neonatal period. The diagnosis is not straightforward in childhood, yet close observation combined with CHA measurement points to the "coat-hanger" sign.

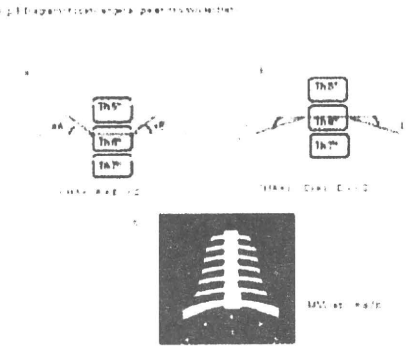

Fig. 1 Diagram of coat-hanger angle and mid/widest ratio
a, b) Coat hanger angle (CHA) refers to the average of the angles between the peak point of both 6th posterior ribs and the horizontal axis. If there is no peak point of the 6th posterior ribs, the center of the ribs is utilized instead. The horizontal axis is defined as a line passing through two points of both 6th cost-vertebral junctions. An upward angle is defined as +, and a downward angle as -. CHA is thought to be a quantitative index of the "coat-hanger" sign.
c) The ratio of mid- to widest thorax (M/W ratio) refers to the ratio of the narrowest diameter of the mid-thorax to the widest diameter of the basal thorax. In most cases with upd(14)pat, the thorax showed medial concavity with the top of approximately the 6th rib (the narrowest mid-thorax) and downward sloping toward the 9th to 11th ribs (the widest basal thorax). M/W ratio is thought to be a quantitative index of dysmorphic bell-shaped thorax.

11x8mm (600 x 600 DPI)